Takatoku M., Uchiyama T., Okamoto S., Kanakura Y., Sawada K., Tomonaga M., Nakao S., Nakahata T., Harada M., Murate T., Ozawa K.	Retrospective nationwide survey of Japanese patients withtransfusion-dependent MDS and aplastic anaemia highlights the negative impact of iron overload on morbidity/mortality.	Eur. J. Hematol		in press	2007
Miyazaki M., Yasunaga J., Taniguchi Y., Tamiya S., Nakahata T., Matsuoka M.	3 Preferential Selection of HTLV-I Provirus Lacking the 5' LTR during Oncogenesis	J. Virol		in press	2007
Tomizawa D., Koh K., Sato T., Kinukawa N., Morimoto A., Isoyama K., Kosaka Y., Oda T., Oda M., Hayashi Y., Eguchi M., Horibe K., Nakahata T., Mizutani S., Ishii E.	Outcome of risk-based therapy for infant acute lymphoblastic leukemia with or without an MLL gene rearrangement, with emphasis on late effects: A final report of two consecutive studies, MLL96 and MLL98, of the Japan Infant Leukemia Study Group.	Leukemia		in press	2007
Saito M., Nishikomori R., Kambe N., Fujisawa A., Tanizaki H., Takeichi K., Imagawa T., Iehara T., Takada H., Matsubayashi T., TanakaH., Kawashima K., Kagami S., Kawai T., Okafuji I., Yoshioka T., Adachi S., Heike T., Miyachi Y., Nakahata T.	Disease-associated CIAS1 mutations induce monocyte death, revealing low-level mosaicism in mutation-negative cryopyrin-associated periodic syndrome patients.	Blood		in press	2007
Shinoda, G., Umeda, K., Heike T., Arai M., Niwa A., Ma F., Suemori H., Luo H.Y., Chui D.H.K., Torii R., Shibuya M., Nakatsuji N., Nakahata, T.	α4-integrin+ endothelium derived from primate embryonic stem cells generates primitive and definitive hematopoietic cells.	Blood	109	2406-2415	2007
Fujisawa A., Kambe N., Saito M., Nishikomori R., Tanizaki H., Kanazawa N., Adachi S., Heike T., Sagara J., Suda T., Nakahata T., Miyachi Y.	Disease-associated mutations in CIAS1 induce cathepsin B-dependent rapid cell death of human THP-1 monocytic cells.	Blood	109	2903-2911	2007
Mamada M., Yorifuji T., Yorifuji J., Kurokawa K., Kawai M., Momoi T., Nakahata T.	Fibrillin I gene polymorphism is associated with tall stature of normal individuals.	Hum. Genet	120(5)	733-735	2007

Ma F., Wang D., Hanada S., Ebihara Y., Kawasaki H., Zaike Y., Heike T., Nakahata T., Tsuji K.	Novel method for efficient production of multipotential hematopoietic progenitors from human embryonic stem cells.	Int. Hematol	85	371-379	2007
Suzuki K, Hiramatsu H, Fukushima-Shintani M, Heike T, Nakahata T.	Efficient Assay for Evaluating Human Thrombopoiesis Using NOD/SCID Mice Transplanted with Cord Blood CD34+ Cells.	Eur J Haematol	78	123-130	2007
Umeda, K., Heike, T., Nakata-Hizume M., Arai M., Shinoda G., Ma F., Suemori H., Luo H.Y., Chui D.H.K., Torii R., Shibuya M., Nakatsuji N., Nakahata T.	Sequential analysis ofα- and β-globin gene expressions during erythropoietic differentiation from primate embryonic stem cells.	Stem Cells	24	2627-2636	2007
Tsuchiya A., Heike T., Fujino H., Shiota M., Umeda K., Yoshimoto M., Matsuda Y., Ichida T., Aoyagi Y., Nakahata T.	Long-term culture of postnatal mouse hepatic stem/progenitor cells and their relative developmental hierarchy.	Stem Cells	25(4)	895-902	2007
Shiota M., Heike T., Haruyama M., Baba S., Tsuchiya A., Fujino H., Koyabashi H., Kato T., Umeda K., Yoshimoto M., Nakahata T.	Isolation and characterization of bone marrow-derived mesenchymal progenitor cells with myogenic and neuronal properties.	Exp. Cell Res	313	1008-1023	2007
Baba S., Heike T., Umeda K., Iwasa T., Kaichi S., Hiraumi Y., Doi H., Yoshimoto M., Kanatsu-Shinohara M., Shinohara T., Nakahata T.	Generation of cardiac and endothelial cells from neonatal mouse testis-derived multipotent germline stem cells.	Stem Cells	25	1375-1383	2007
Tono C., Takahashi Y., Terui K., Sasaki S., Kamio T., Tandai T., Sato T., Kudo K., Toki T. Tachibana N., Yoshioka T., Nakahata T., Morio T., Nishikomori R., Ito E.	Correction of immunodeficiency associated with NEMO mutation by umbilical cord blood transplantation using a reduced-intensity conditioning regimen.	Bone Marrow Transplant	39	801-4	2007

Baba S., Heike T., Umeda K., Doi H., Iwasa T., Nakajima H., Lin X., Matsuoka S., Komeda M., Nakahata T.	Flk1+ Cardiac Stem/Progenitor Cells Derived from ES Cells Improve the Cardiac Function of Dilated Cardiomyopathy Mice.	Cardiovascular Res	76	119-131	2007
Yamamura K., Ohishi K., Katayama N., Kato K., Shibasaki T., Sugimoto Y., Miyata E., Shiku H., Masuya M., Nishioka J., Nobori T., Nishikawa M., Inagaki Y., Hiramatsu H., Nakahata T.	Notch ligand Delta-1 differentially modulates the effects of gp130 activation on interleukin-6 receptorα-positive and -negative human hematopoietic progenitors.	Cancer Sci	98(10)	1597-1603	2007
Yokota, A., Kimura, S., Masuda, S., Ashihara, E., Kuroda, J., Sato, K., Kamitsuji, Y., Kawata, E., Deguchi, Y., Urasaki, Y., Terui, Y., Ruthardt, M., Ueda, T., Hatake, K., Inui, K., and Maekawa, T	INNO-406, a novel BCR-ABL/Lyn dual tyrosine kinase inhibitor, suppresses the growth of Ph+ leukemia cells in the central nervous system and cyclosporine A augments its *in vivo* activity.	Blood	109(1)	306-314	2007
Horie, N., Murata, H., Kimura, S., Takeshita, H., Sakabe, T., Matsui, T., Maekawa, T., Kubo, T., Fushiki, S.	Combined effects of a third-generation bisphosphonate, zoledronic acid with other anti-cancer agents against osteosarcoma.	Brit J Cancer	96(2)	255-261	2007
Ashihara, E., Tsuji, H., Sakashita, Y., Haga, H., Yurugi, K., Kimura, S., Egawa, H., Manabe, T., Uemoto, S., Maekawa. T.	Anti-donor antibody in patients receiving ABO-identical and HLA-mismatched living donor liver transplants: effect on survival	Transplantation	83(4)	506-509	2007
Uchida, R., Ashihara, E., Sato, K., Kimura, S., Kawata, E., Taniguchi, K., Okamoto, M., Shimura, K., Kiyono, Y., Shimazaki, C., Taniwaki, M., Maekawa, T.	γδT cells kill myeloma cells by sensing mevalonate metabolites and ICAM-1 molecules on cell surface.	Biochem Biophys Res Commun	354(2)	613-618	2007
Egawa, H., Ohmori, K., Haga, H., Tsuji, H., Yurugi, K., Miyagawa-Hayashino, A., Oike, F., Fukuda, A., Yoshizawa, J., Takada, Y., Tanaka, K., Maekawa, T., Ozawa, K., Uemoto, S.	B-cell surface marker analysis for improvement of rituximab prophylaxis in ABO-incompatible adult living donor liver transplantation.	Liver Transpl	13(4)	579-588	2007

Yurugi, K., Kimura, S., Ashihara, E., Tsuji, H., Kawata, E., Kamitsuji, Y., Hishida, R., Takegawa, R, Egawa, H., Maekawa, T.	Rapid and accurate measurement of anti-A/B IgG antibody in ABO-unmatched living donor liver transplantation by surface plasmon resonance.	Transfusion Med	17(2)	97-106	2007
Wada, M., Kawahito, Y., Kimura, S., Kohno, M., Ishino, H., Kimura, M., Omoto, A., Yamamoto, A., Hamaguchi, M., Tsubouchi, Y., Ashihara, E., Tokunaga, D., Hojo, T., Maekawa, T., Yoshikawa, Y.	Small interfering RNA targeting PLK-1 induces the apoptosis of synoviocytes of rheumatoid arthritis.	Biochem Biophys Res Commun	357(2)	353-359	2007
Sakashita, H., Haga, H., Ashihara, E., Wen, M-C., Tsuji, H., Miyagawa-Hayashino, A., Egawa, H., Takada, Y., Maekawa, T., Uemoto, S., Manabe, T.	Significance of C4d staining in ABO-identical/compatible liver transplantation.	Modern Pathol	20(6)	676-684	2007
Munaka, T., Abe, H., Kanai, M., Sakamoto, T., Nakanishi, H., Shoji, S., Kimura, S., Maekawa, T., Murakami, A.	Real-time monitoring of antibody secretion from B-cells on a microchip stimulated with a minute amount of mitogen.	Analyst	132(6)	512-514	2007
Yuasa, T., Kimura, S., Ashihara, E., Habuchi, T., Maekawa, T.	Multiplicity for anti-cancer activity with zoledronic acid.	Curr Med Chem (review)	14(20)	2126-2135	2007
Kuroda, J., Kimura, S., Strasser, A., Andreeff, M., O'Reilly, L.A., Ashihara, E., Kamitsuji, Y., Yokota, A., Kawata, E., Deguchi, Y., Takeuchi, M., Tabe, Y., Taniwaki, M., Maekawa, T.	Dual molecular targeting by INNO-406, a second generation Bcr-Abl inhibitor, and ABT737, an inhibitor of anti-apoptotic Bcl-2 proteins against Bcr-Abl-positive leukemia.	Cell Death Diff	14(9)	1667-77	2007

Maekawa, T., Ashihara, E., Kimura, S.	The Bcr-Abl tyrosine kinase inhibitor imatinib and promising new agents against Philadelphia chromosome positive leukemias.	Int J ClinOncol(review)	12(5)	327-340	2007
Kawata, E., Kuroda, J., Wada, K., Kamiuchi, K., Nakayama-Harusato, I., Kimura, S., Maekawa, T., Kitagawa, Y.	Hypereosinophilic syndrome accompanied with Buerger's disease-like femoral arterial occlusion.	Intern Med	46(23)	1919-1922	2007
Horie, N., Murata, H., Nishigaki, T., Segawa, H., Yuasa, T., Kimura, S, Maekawa, T., Fushiki, S., Kubo, T.	The third-generation bisphosphonates inhibit tumor proliferation and induce apoptosis in murine osteosarcoma in vitro.	Cancer Lett		in press	2007
Kageyama, S., Iwaki, H., Inoue, H., Isono, T., Yuasa,. T., Nogawa, M., Maekawa, T., Ueda, M., Kajita, Y., Ogawa, O., Toguchida, J., Yoshiki, T.	A novel tumor-related protein, C7orf24, identified by proteome differential display of bladder urothelial carcinoma.	Proteomics		in press	2007
Kuroda, J., Kimura, S., Kamitsuji, Y., Yokota, A., Ashihara, E., Kawata, E., Takeuchi, M., Tanaka, R., Tanaka, H., Matsumoto, Y., Andreeff, M., Taniwaki, M., Maekawa, T.	ABT-737 is a useful component of combinatory chemotherapies for chronic myelogenous leukaemias with diverse drug resistance mechanisms	Brit J Haematol		in press	2007
Deguchi, Y., Kimura, S., Ashihara, E., Niwa, T., Hodohara, K., Fujiyama, Y., Maekawa, T.	Comaprison of imatinib, dasatinib, nilotinib, and INNO-406 in imatinib-resistant cell liness	Leuk Res		in press	2007
Kitawaki, T., Kadowaki, N., Kondo, T., Ishikawa, T., Ichinohe, T., Teramukai, S., Fukushima, M., Kasai, Y., Maekawa, T., Uchiyama, T.	Potential of dendritic cell immunotherapy for relapse after allogeneic hematopoietic stem cell transplantation, shown by WT1 peptide- and keyhole limpet hemocyanin-pulsed, donor-derived dendritic cell vaccine for acute myeloid leukemia.	Am J Hematol		in press	2007

Morinaga, K., Yamauchi, T., Kimura, T., Maekawa, T., Ueda, T.	Overcoming imatinib resistance using Src inhibitor CGP76030, Abl inhibitor nilotinib, and Abl/Lyn inhibitor INNO-406 in newly established K562 variants with BCR-ABL gene amplification	Int J Cancer		in press	2007
Tanaka, R., Kuroda, J., Stevenson, W., Ashihara, E., Ishikawa, T., Taki, T., Kobayashi, Y., Kamitsuji, Y., Kawata, E., Takeuchi, M., Murotani, Y., Yokota, A., Hirai, M., Majima, S., Taniwaki, M., Maekawa, T., Kimura, S.	Detection of the V617F mutation in JAK2 using a novel, fully automated, SNP super-rapid detector.	Leuk Res		in press	2008
Shimura, K., Ashihara, E., Shimazaki, C., Matsunaga, S., Taniguchi, K., Uchiyama, H., Matsumoto, Y., Kimura, S., Matsubara, H., Taniwaki, M., Maekawa, T.	Kinetics of circulating endothelial progenitors in patients with sclerodermatous chronic graft-versus-host disease	Biol Blood Marrow Transplant		in press	2008
Muramatsu, H., Kimura, S., Ichinohe, T., Ashihara, E., Ishikawa, T., Maekawa, T., Uchiyama, T.	Consulting clinic for related family donors in hematopoietic stem cell transplantation	Bone Marrow Transplant		in press	2008
Masaie H, Oritani K, Yokota T, Takahashi I, Shirogane T, Ujiie H, Ichii M, Saitoh N, Maeda T, Tanigawa R, Oka K, Hoshida Y, Tomiyama Y, Kanakura Y.	Adiponectin binds to chemokines via the globular head and modulates interactions between chemokines and heparan sulfates.	Exp Hematol	35	947-956	2007
Tanaka H, Matsumura I, Kanakura Y.	Potential Target Molecules for Ex Vivo Expansion of Hematopoietic Stem Cells and Their Roles in Normal Hematopoesis.	J. Stem Cells	2(3)	167-183	2007
Ishiko J, Mizuki M, Yasumi M, Ujiie H, Nakamichi I, Aozasa K, Kanakura Y.	An indolent subtype of "intravascular lymphoma": A case with a 3-year history of LDH elevation.	Leuk Lymphoma	48	1872-1874	2007

Nakamichi I, Tomita Y, Zhang B, Sugiyama H, Kanakura Y, Fukuhara S, Hino M, Kanamaru A, Ogawa H, Aozasa K.	Correlation between promoter hypermethylation of GSTP1 and response to chemotherapy in diffuse large B cell lymphoma.	Ann Hematol	86	557-564	2007
Nojima J, Sakudo A, Hakariya Y, Kuratsune H, Watanabe Y, Kanakura Y, Ikuta K.	Spectroscopic diagnosis of anti-phospholipid antibodies by visible and near-infrared spectroscopy in SLE patients'plasma samples.	Biochem Biophys Res Commun	362	522-524	2007
Yamauchi A, Fujita S, Ikeda J, Nakamichi I, Fukuhara S, Hino M, Kanakura Y, Ogawa H, Sugiyama H, Kanamaru A, Aozasa K.	Diffuse large B-cell lymphoma in the young in Japan: A study by the Osaka Lymphoma Study Group.	Am J Hematol	82	893-897	2007
Takatoku M, Uchiyama T, Okamoto S, Kanakura Y, Sawada K, Tomonaga M, Nakao S, Nakahata T, Harada M, Murate T, Ozawa K	Retrospective nationwide survey of Japanese patients with transfusion-dependent MDS and aplastic anemia highlights the negative impact of iron overload on morbidity/mortality.	Eur J Haematol	78	487-494	2007
Sugita S, Shimizu N, Kawaguchi T, Akao N, Morio T, Mochizuki M.	Identification of human herpesvirus 6 variant A in a patient with unilateral panuveitis.	Arch.of Ophthalmol		in press	2007
Kido S, Sugita S, Horie S, Miyanaga M, Miyata K, Shimizu N, Morio T, Mochizuki M.	Association of varicella-zoster virus (VZV) load in the aqueous humor with clinical manifestations of anterior uveitis in herpes zoster ophthalmicus and zoster sine herpete.	Br. J. Ophthalmol.		in press	2007

Takahashi H, Sugita S, Shimizu N, Mochizuki M.	A high viral load of EBV DNA in ocular fluids in a HLA-B27 negative acute anterior uveitis patient with psoriasis.	Jap.J. Ophthalmol.		in press	2007
Watanabe S, Terashima K, Ohta S, Horibata S, Yajima M, Shiozawa Y, Dewan Z, Yu Z, Ito M, Morio T, Shimizu N, Honda M, and Yamamoto N.	Hematopoietic stem cell-engrafted NOD/SCID/IL2R□null mice develop human lymphoid system and induce long-lasting HIV-1 infection with specific humoral Immune Responses.	Blood	109	212-218	2007
Kawaguchi T, Sugita S, Shimizu N and Mochizuki M.	Kinetics of aqueous flare, intraocular pressure and virus-DNA copies in a patient with cytomeralovirus iridocyclitis without retinitis.	Int. Ophthalmo	27	383- 386	2007
Watanabe S, Ohta S, Yajima M, Terashima K, Ito M, Mugishima H, Fujiwara S, Shimizu K, Honda M, Shimizu N and Yamamoto N.	Humanized NOD/SCID/IL2Rgnull mice transplanted with hematopoietic stem cell under non-myeloablative condition show prolonged life spans and allow detailed analysis of HIV-1 pathogenesis.	J.Virol	81	13259-13264	2007
Kanno H., .Watabe S, Shimizu N. and Sawai T.	Adhesion of Epstein-Barr virus-positive natural killer cell lines to cultured endothelial cells stimulated with inflammatory cytokines.	Clin.Exp.Immunol	151	519-527	2007

研究成果の刊行に関する一覧表(和文)					
発表者氏名	論文タイトル名	発表誌名	巻名	ページ	出版年
河井昌彦、水本洋、丹羽房子、中畑龍俊	早期新生児期のDIC診断基準の考案-プロトロンビン時間を重視した診断基準作成の試み-	日本周産期・新生児医学会雑誌	43	1(10-14)	2007
森口直彦、石田也寸志、加藤剛史、鬼頭敏幸、篠田邦大、水江伸夫、西村真一郎、中畑龍俊	小児急性リンパ性白血病治療中の重症感染症の検討	日本小児血液学会雑誌	21	19-24	2007
松原康策、金岡裕夫、奥村光祥、黒須英雄、前田真治、浜口賢子、南部光彦、河井昌彦、中畑龍俊	2000年ー2004年の早発型・遅発型B群溶連菌感染症頻度の推定-未熟児新生児医療研究会調査から-	日本周産期・新生児医学会雑誌	43(3)	701-705	2007
中畑龍俊	臍帯血／骨髄造血幹細胞の増幅	バイオ医薬品の開発と品質・安全性確保第6節		530-536	2007
田中宏和、伊藤仁也、丸山京子、中畑龍俊	Ex vivo増幅造血幹／前駆細胞の臍帯血移植への応用	再生医療11月号	6(4)	61-66	2007
中畑龍俊、梅田雄嗣	血球系の再生医療	Medical Science Digest	33(14)	20-24	2007
前川　平	「日本における抗がん剤の臨床開発」欧米からの周回遅れを挽回するために—学の立場から—：イマチニブ耐性CMLに対する新規Bcr-Abl/Lynチロシンキナーゼ阻害剤の開発を例にあげて	第一回抗悪性腫瘍薬開発フォーラム、癌と化学療法	34(2)	301-304	2007

前川　平	輸血・成分輸血．内科学（第九版）．（杉本恒明、矢崎義雄　総編集）	朝倉書店、東京		166-174	2007
前川　平	Cell Therapy-基礎研究から臨床応用へ	BioClinica	22(12)	1036-1037	2007
笠井泰成、前川　平	細胞プロセシングセンター．遺伝子MOOK別冊「歩みつづける細胞移植療法の実際?再生医療の実現に向けた科学・技術と周辺要素の理解−」	メディカルドゥ、大阪		印刷中	2007
前川　平	輸血関連急性肺障害の予防と治療方針は？　EBM−血液疾患の治療．（押見和夫、別所正美、岡本真一郎、加藤淳　編集）	中外医学社、東京		568-573	2007
笠井泰成、前川　平	再生医学のいま　臨床応用に向けて−その基盤整備の重要性−	治療	89(10)	2888-2893	2007
笠井泰成、前川　平	本邦における安全な細胞療法の実施に向けて	血液フロンティア	18(1)	69-73	2008
金倉　譲	総論：血液疾患領域の最近の進歩 -分子病態に基づく診断と治療-	BIO Clinica	22	296-297	2007
松村　到，金倉　譲	新規チロシンキナーゼ阻害剤の開発と臨床試験の現状	血液・腫瘍科	54	158-166	2007

松村　到，金倉　譲	造血器腫瘍　基礎・臨床領域における最新の研究動向　白血病関連遺伝子	日本臨床	65	100-104	2007
松村　到，金倉　譲	ファルネシル化阻害剤	医学のあゆみ	220	765-770	2007
松村　到，金倉　譲	癌幹細胞と分子標的療法	Biotherapy	21	209-216	2007
松村　到，金倉　譲	データで読み解く内科疾患　再生不良性貧血	総合臨床	56	539-543	2007
松村　到，金倉　譲	Hyper Eoninophilic Sndrome：病態と治療	Bio Clinica	22	68-73	2007
松村　到，金倉　譲	造血幹細胞を制御するシグナル伝達分子	血液・腫瘍科	54	635-640	2007
松村　到，金倉　譲	急性白血病の分類と診断 -臨床医がおさえておきたい重要事項-	Medical Practice	24	1922-1928	2007
松村　到，金倉　譲	新しい血小板増多因子	血液フロンティア	17	106-112	2007
松村　到，金倉　譲	血球分化に伴う細胞周期制御とそのメカニズム	血液フロンティア	17	43-50	2007
松村　到，金倉　譲	造血のしくみ．内科学 第９版（杉本恒明，矢崎義雄編）	朝倉書店，東京		1555-1559	2007
水木満佐央，金倉　譲	慢性骨髄性白血病．内科学 第９版（杉本恒明，矢崎義雄編）	朝倉書店，東京		1656-1659	2007

西村純一，金倉　譲	発作性夜間ヘモグロビン尿症のクローン拡大の機序. Annual Review　血液2007（高久史麿，溝口秀昭，坂田洋一，金倉　譲，小島勢二編）	中外医学社，東京		69-77	2007
西村純一，金倉　譲.	PNHの遺伝子異常	血液フロンティア	17	88-95	2007
田中宏和，伊藤仁也	造血幹細胞の体外増幅	血液・腫瘍科	55	40-47	2007
田中宏和，伊藤仁也，丸山京子，中畑龍俊	Ex vivo増幅造血幹/前駆細胞の臍帯血移植への応用	再生医療	6	61-66	2007
近藤　礎，田墨恵子，糀　桂子，松村菜津子，竹上　学，黒川信夫，金倉譲，野口眞三郎，水木満佐央	オーダリングシステム型外来化学療法部の現況と問題点	癌と化学療法	34	1264-1266	2007

Ⅵ. 研究成果の刊行物・印刷物

α4-Integrin$^+$ endothelium derived from primate embryonic stem cells generates primitive and definitive hematopoietic cells

Gen Shinoda,[1] Katsutsugu Umeda,[1] Toshio Heike,[1] Masato Arai,[1] Akira Niwa,[1] Feng Ma,[1] Hirofumi Suemori,[2] Hong Yuan Luo,[3] David H. K. Chui,[3] Ryuzo Torii,[4] Masabumi Shibuya,[5] Norio Nakatsuji,[6] and Tatsutoshi Nakahata[1]

[1]Department of Pediatrics, Graduate School of Medicine, [2]Laboratory of Embryonic Stem Cell Research, Stem Cell Research Center, Institute for Frontier Medical Sciences, and [6]Department of Development and Differentiation, Institute for Frontier Medical Sciences, Kyoto University, Japan; [3]Department of Medicine, Boston University School of Medicine, MA; [4]Research Center for Animal Life Science, Shiga University of Medical Science, Japan; [5]Division of Genetics, Institute of Medical Science, University of Tokyo, Japan

The mechanism of commencement of hematopoiesis in blood islands of the yolk sac and the aorta-gonad-mesonephros (AGM) region during primate embryogenesis remains elusive. In this study, we demonstrated that VE-cadherin$^+$CD45$^-$ endothelial cells derived from nonhuman primate embryonic stem cells are able to generate primitive and definitive hematopoietic cells sequentially, as revealed by immunostaining of floating erythrocytes and colony-forming assay in cultures. Single bipotential progenitors for hematopoietic and endothelial lineages are included in this endothelial cell population. Furthermore, hemogenic activity of these endothelial cells is observed exclusively in the α4-integrin$^+$ subpopulation; bipotential progenitors are 4-fold enriched in this subpopulation. The kinetics of this hemogenic subpopulation is similar to that of hemogenic endothelial cells previously reported in the yolk sac and the AGM region in vivo in that they emerge for only a limited time. We suggest that VE-cadherin$^+$CD45$^-$α4-integrin$^+$ endothelial cells are involved in primitive and definitive hematopoiesis during primate embryogenesis, though VE-cadherin$^-$CD45$^-$α4-integrin$^+$ cells are the primary sources for primitive hematopoiesis. (Blood. 2007;109: 2406-2415)

Introduction

During mammalian embryogenesis, hematopoietic system development undergoes 2 distinct phases, primitive hematopoiesis and definitive hematopoiesis. The phases are distinguished from each other by 2 characteristics. First, primitive hematopoiesis originates exclusively in the extraembryonic yolk sac and is transient, whereas definitive hematopoiesis occurs in the intraembryonic aorta-gonad-mesonephros (AGM) region, shifts to the liver, spleen, and bone marrow, and persists for life. Evidence also indicates that the yolk sac serves as a source of initial definitive hematopoietic progenitors in humans, as it does in mice.[1,2] Second, in primates, primitive erythrocytes are larger and primarily synthesize embryonic globin chains (ζ, ε), whereas definitive erythrocytes are smaller and synthesize fetal/adult globin chains (α, γ, and β).[3,4] Because the embryonic–fetal globin switch (ζ → α and ε → γ) occurs gradually in the fetal liver, embryonic and fetal globins are expressed during the transition from primitive to definitive hematopoiesis. However, adult β-globin is predominantly expressed in definitive erythrocytes and is only marginally expressed, if at all, in primitive erythrocytes.

The existence of the hemangioblast, the common precursor of hematopoietic and endothelial lineages, has been discussed for many years. Histologically, hematopoietic and endothelial cells develop from the same clusters of mesoderm in yolk sac blood islands.[5,6] In addition to the shared expression of several markers, gene-targeting experiments on vascular endothelial growth factor receptor-2 (VEGFR-2) disclose a common developmental pathway between both cell types.[7,8] Furthermore, a single common precursor generates both cell types during in vitro differentiation of mouse embryonic stem cells (ESCs).[9] Recent evidence shows that intraembryonic hematopoiesis originates from the ventral endothelial walls of the dorsal aorta and the umbilical and vitelline arteries, challenging the concept of common progenitors.[10-16] Endothelial cells capable of generating hematopoietic cells are designated "hemogenic endothelium."[17,18] Earlier studies using mouse embryos demonstrate that endothelial cells in the yolk sac are able to generate hematopoietic cells, which is also suggested by some reports on human embryos.[12,15,16] The embryos were used, however, at the stage after vascular connection between the yolk sac and the embryo proper. Hence, though it is established that definitive hematopoiesis in the AGM region originates at least in part in endothelial cells, the origin of primitive/definitive hematopoiesis in the yolk sac is still unclear.

The aims of this study were to investigate the relationship between hemogenic endothelium and primitive/definitive hematopoiesis in primates and to identify markers of the hemogenic endothelium. Analyses using primate materials are necessary because a number of differences occur in hematopoietic development between mice and primates (human and monkey). These studies are difficult to perform because of the poor availability of primate embryos and the ethical limitations involved in their use. Recently established primate ESC lines[19-22] are promising alternative tools in developmental biology and regenerative medicine. We previously showed the development of hematopoietic and

Submitted June 26, 2006; accepted October 25, 2006. Prepublished online as *Blood* First Edition Paper, November 7, 2006; DOI 10.1182/blood-2006-06-031039.

The online version of this article contains a data supplement.

The publication costs of this article were defrayed in part by page charge payment. Therefore, and solely to indicate this fact, this article is hereby marked "advertisement" in accordance with 18 USC section 1734.

endothelial cells when cynomolgus monkey ESCs were cocultured with OP9 stromal cells, which was enhanced by exogenous vascular endothelial growth factor (VEGF).[23,24] In our coculture system, the transition from primitive to definitive hematopoiesis was induced, as confirmed by globin switching.[25] Here, we examined the hematopoietic potential of endothelial cells in our coculture system and demonstrated that isolated VE-cadherin$^+$CD45$^-$ endothelial cells generated primitive and definitive hematopoietic cells based on morphologic and globin expression analyses. We used α4-integrin, an effective marker of the hemogenic population among endothelial cells in mouse embryos and in in vitro differentiating ESCs,[26] as a candidate marker of hemogenic endothelial cells in primates. Our data show that the capacity for primitive and definitive hematopoiesis resides exclusively in the α4-integrin$^+$ subpopulation among ESC-derived endothelial cells, though VE-cadherin$^-$CD45$^-$α4-integrin$^+$ cells are primary sources for primitive hematopoiesis.

Materials and methods

Maintenance of cell lines

The ESC line CMK6, established from cynomolgus monkey blastocysts, was maintained as described .[19] The GFP-transfected ESC subline[27] was applied to exclude OP9 cells in some experiments. OP9 stromal cells, a kind gift from Dr Hiroaki Kodama, were maintained as reported previously.[24]

Antibodies

Primary antibodies used in this study included mouse anti–human CD34-phycoerythrin (PE), CD41a-allophycocyanin (APC), α4-integrin-PE, endothelial nitric oxide synthase (eNOS) monoclonal antibodies (mAbs; BD PharMingen, San Diego, CA), mouse anti–human CD31-PE (eBioscience, San Diego, CA), rabbit anti–human von Willebrand factor (VWF; Nichirei, Tokyo, Japan), mouse anti–human CD45 and CD41 mAbs (Dako, Kyoto, Japan), mouse anti–human VE-cadherin mAb (Immunotech, Marseille, France), mouse anti–human β-globin and γ-globin mAbs (Santa Cruz Biotechnology, Santa Cruz, CA), rabbit anti–human hemoglobin (Hb) polyclonal Ab (Cappel, Aurora, OH), and their corresponding IgG1 isotype controls (BD PharMingen and Dako). Mouse anti–human VE-cadherin mAb (BD PharMingen) and its corresponding IgG1 isotype control were labeled with Alexa Fluor 647 monoclonal antibody labeling kit (Invitrogen, Carlsbad CA). Mouse anti–human ε-globin and ζ-globin and mouse anti–human VEGFR-2 mAbs were used, as reported previously.[28-30] Mouse anti–human α-globin mAb was established in the laboratory of D.H.K.C. All primary antibodies against human antigens used in this study cross-reacted with cynomolgus monkey compartments.[23,24] Secondary Abs included Cy3-conjugated, horseradish peroxidase (HRP)–conjugated, or alkaline phosphatase (ALP)–conjugated donkey anti–mouse IgG, fluorescein isothiocyanate (FITC)–conjugated donkey anti–rabbit IgG (Jackson ImmunoResearch Laboratories, West Grove, PA), PE-conjugated goat anti–mouse IgG (Dako), and FITC- or APC-conjugated goat anti–mouse IgG (BD PharMingen).

In vitro differentiation of primate ESCs

Initial differentiation of ESCs and cell sorting were based on earlier experiments.[23,24] Briefly, trypsin-treated undifferentiated ESCs were transferred onto OP9 cells and cultured in the presence of 20 ng/mL VEGF (R&D Systems, Minneapolis, MN).

For hematopoietic differentiation, cells sorted on day 10 were cultured in α-MEM (Gibco BRL, Grand Island, NY) containing 10% fetal calf serum (FCS; Sigma, St Louis, MO), 50 μM 2-mercaptoethanol (ME), and a mixture of 10 ng/mL G-CSF, 2 U/mL EPO, 20 ng/mL IL-3, 100 ng/mL SCF, and 10 ng/mL TPO (hematopoietic cytokine mixture; all were provided by Kirin Brewery, Tokyo, Japan). For endothelial differentiation, sorted cells were cultured on OP9 cells in α-MEM containing 10% FCS, 50 μM 2-ME, and 20 ng/mL VEGF or were seeded onto type I collagen-coated plates in medium (CS-C Complete Medium; Cell Systems, Kirkland, WA) supplemented with 20 ng/mL VEGF.

Fluorescence-activated cell sorter analysis and cell sorting

Staining procedures, FACS analysis, and cell sorting were performed as described earlier.[23,24] For multicolor staining, single-cell suspensions were initially stained with unconjugated anti–CD45 mAb or its corresponding IgG1 isotype control, followed by FITC-, PE-, or APC-conjugated goat anti–mouse IgG. The cells were washed twice, incubated with robust mouse IgG to prevent redundant secondary Abs from reacting with other mouse mAbs, and stained with fluorochrome-conjugated mAbs, including CD34, VE-cadherin, and α4-integrin. Dead cells were excluded by propidium iodide (PI) staining. Samples were analyzed with the use of FACSCalibur and Cell Quest software (Becton Dickinson, San Jose, CA) or were sorted on a FACSVantage SE (Becton Dickinson).

Immunochemistry and acetylated low-density lipoprotein (Ac-LDL) uptake

May-Giemsa staining, immunostaining of floating erythrocytes and endothelial colonies, and DiI-Ac-LDL incorporation assay were performed as described previously.[23,24] VE-cadherin$^+$CD45$^-$ cells isolated on day 10 or their progeny were cytospun onto glass slides, fixed, and permeabilized in a staining procedure similar to that for hemoglobin.[24] Cells were initially stained with anti–VE-cadherin mAb and Cy3-conjugated donkey anti–mouse IgG, followed by double staining with various Abs using the Vector MOM kit (Vector Laboratories, Burlingame, CA), visualized with the TSA fluorescence systems kit (PerkinElmer Life Sciences, Boston, WA), and counterstained with Hoechst 33342. Fluorescence was detected on an Olympus IX70 microscope (Olympus, Tokyo, Japan) that was equipped with 4 ×/0.13 NA, 10 ×/0.30 NA, and 20 ×/0.40 NA objectives, and images were obtained with an AxioCam photomicroscope and AxioVision software version 3.0.6 SP4 (Carl Zeiss Vision, Hallbergmoos, Germany). Images were processed using Adobe Photoshop 6.0 (Adobe Systems, San Diego, CA).

Colony-forming assays for primitive and definitive cells

Colony-forming assays were performed as described elsewhere.[24,31] Briefly, for colonies consisting of primitive cells, sorted cells in each subpopulation were reseeded on OP9 layers, and the medium was replaced with methylcellulose-containing medium supplemented with 30% FCS and hematopoietic cytokine mixture on the following day. For colonies composed of definitive cells, we initially trypsinized cells and allowed OP9 stromal cells to adhere to culture dishes to exclude OP9. Resultant floating fractions were transferred to new Petri dishes with methylcellulose-containing medium supplemented with 30% FCS and hematopoietic cytokine mixture and were cultured at 37°C, 5% CO_2, in a humidified incubator. Colonies were scored using an inverted microscope[24,32,33] after 7 days for primitive cells and 14 days for definitive cells. Colonies were selected for cytospin and further staining. All assays were performed at a concentration of 0.5-2 × 10^4 cells/mL in duplicate or triplicate.

Single-cell deposition assay for hematopoietic and endothelial differentiation

Single-cell deposition assay was performed as described earlier.[23] Briefly, single-sorted cells were deposited in individual wells of 96-well plates with confluent OP9 layers and were cultured in α-MEM containing 10% FCS, 50 μM 2-ME, and hematopoietic cytokine mixture for 7 days. Each well was initially stained with a mixture of anti-CD45, anti-CD41, and anti–γ-globin mAbs, followed by HRP-conjugated donkey anti–mouse IgG for hematopoietic lineage detection, and each was double stained with anti–VE-cadherin mAb using the Vector MOM kit (Vector), followed by ALP-conjugated donkey anti–mouse IgG for endothelial lineage detection.

Reverse transcription–polymerase chain reaction

We performed RNA isolation and RT-PCR according to previously established protocols.[23,24] Samples were initially denatured at 94°C for 5 minutes, followed by 35 to 40 amplification reactions consisting of 94°C for

1 minute (denaturing), 60°C to 62°C for 1 minute (annealing), 72°C for 1 minute (extension), and a final extension at 94°C for 7 minutes. Primers for *eNOS*, *SCL*, *GATA-2*, *RUNX1*, and *GAPDH* are described elsewhere.[23,34] Other primers used included α4-integrin (434 bp) (sense, 5′-AGATGGGATCTCGTCAACCTTC-3′; antisense, 5′-TGGACACCTGTATGCTTCCTG-3′), *VWF* (472 bp) (sense, 5′-GGGACCTTTCGGATCCTAGTG-3′; antisense, 5′-AGGAGGAATCCACCATCGTC-3′), and mouse β-actin (613 bp) (sense, 5′-ATCCTGACCCTGAAGTACCCCATT-3′; antisense, 5′-CCAAGAAGGAAGGCTGGAAAAGAG-3′). cDNA from adult cynomolgus monkey BM cells, human erythroblastic cells (K562), and human umbilical vein endothelial cells were used as positive controls, and mouse OP9 cells were used as a negative control. For semiquantitative comparison, samples were normalized by dilution to produce equivalent signals for *GAPDH*.

Statistical analysis

Statistical analyses were conducted using the Student *t* test or Fisher exact test. Statistical significance was defined as a *P* value below .05.

Results

Development of primate ESC-derived VE-cadherin$^+$CD45$^-$ endothelial cells

Initially, we investigated when cells positive for hematopoietic or endothelial markers emerged during ESC differentiation. GFP-transfected ESCs were induced to differentiate by coculture with OP9 stromal cells in the presence of exogenous VEGF. Sequential FACS analysis for various surface markers was performed, and the percentage of positive cells among viable GFP$^+$ cells was quantified (Figure 1A). Undifferentiated ESCs expressed low levels of VEGFR-2 but not other hematopoietic or endothelial markers, such as CD31, CD34, VE-cadherin, CD41a, or CD45 (Figure 1B). VEGFR-2 was down-regulated by day 4 of culture but subsequently was re-expressed on a fraction of differentiating cells. CD31$^+$, CD34$^+$, and VE-cadherin$^+$ cells initially appeared on day 6, and CD41a$^+$ and CD45$^+$ cells appeared on day 12. Thus, cells positive for VE-cadherin, an endothelial marker, emerged in the OP9 coculture earlier than those positive for the hematopoietic marker CD41a or CD45.

VE-cadherin belongs to the cadherin family of adhesive transmembrane proteins and is expressed solely in endothelial cells.[35] The protein is additionally detected in all developing vessels from early embryonic stages.[36] To date, VE-cadherin has been used for the isolation of cells committed to endothelial lineage as an endothelial-specific marker.[15,16,26,37] Accordingly, we used anti–VE-cadherin and CD45 mAbs to purify endothelial cells and exclude hematopoietic cells (Figure 1C). Indeed, isolated VE-cadherin$^+$CD45$^-$ cells on day 10 exclusively coexpressed CD31 and CD34 but not CD41a (Figure 1D). Moreover, all VE-cadherin$^+$CD45$^-$ cells on day 10 had Ac-LDL uptake capacity and expressed VEGFR-2 and eNOS but not Hb (Figure 1E-I). On the other hand, only 27.4% ± 7.8% cells expressed VWF (n = 3) (Figure 1J), suggesting that most were functionally immature. Our results indicated that VE-cadherin$^+$CD45$^-$ cells generated on day 10, before the emergence of hematopoietic cells, had several endothelial characteristics.

VE-cadherin$^+$CD45$^-$ population generates hematopoietic and endothelial cells

To determine the hematoangiogenic capacity of isolated VE-cadherin$^+$CD45$^-$ cells, VE-cadherin$^+$CD45$^-$ and VE-cadherin$^-$CD45$^-$ cells were reseeded separately onto fresh, confluent OP9 cells and cultured with hematopoietic cytokine mixture (see "Materials and methods") for hematopoietic differentiation or with VEGF for endothelial differentiation.

In hematopoietic differentiation cultures, adherent hematopoietic clusters initially emerged from the VE-cadherin$^+$CD45$^-$ population at approximately day 10 + 3 (3 days after sorting on day 10) (Figure 2A) and covered large areas of OP9 stromal layers by day 10 + 21 (Figure 2B). In contrast, adherent hematopoietic clusters from the VE-cadherin$^-$CD45$^-$ population were rare and small and disappeared by day 10 + 12 (data not shown). Under hematopoietic differentiation conditions, the numbers of CD45$^+$ and CD45$^+$CD34$^+$ hematopoietic

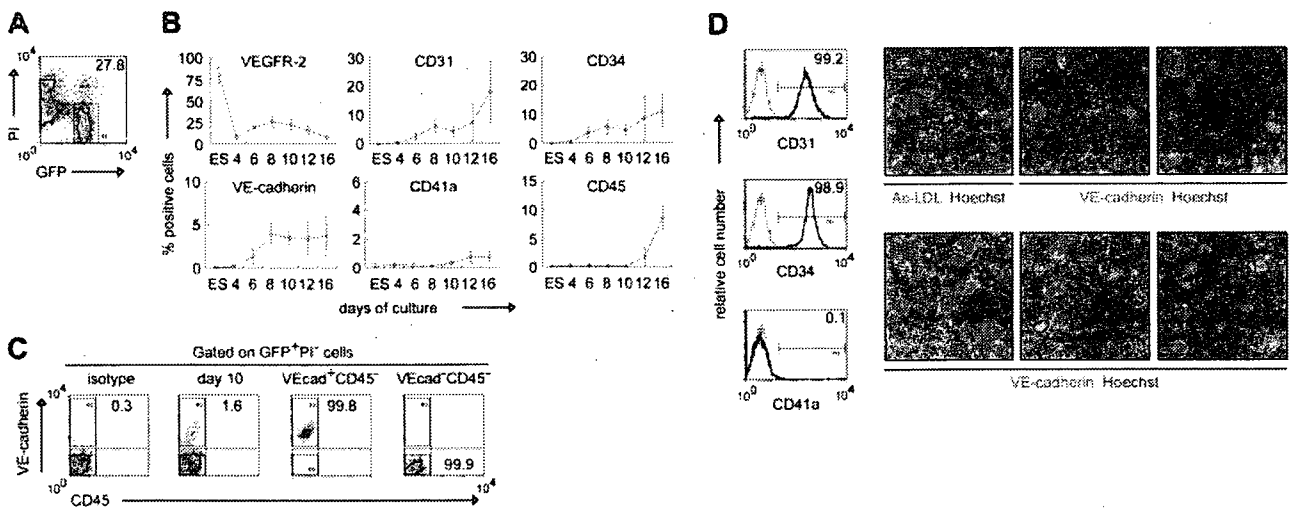

Figure 1. ESC-derived VE-cadherin$^+$CD45$^-$ cells have endothelial properties. Undifferentiated GFP-transfected ESCs (ES) and subsequent differentiating cells were analyzed by FACS. GFP$^+$PI$^-$ cells were gated as ESC-derived viable cells. (A) Percentage of gated cells among the total cells is specified. (B) Sequential analysis of the percentage of cells positive for each antigen among ESC-derived viable cells. Data are presented as mean ± SD of 3 independent experiments. (C) VE-cadherin$^+$CD45$^-$(VEcad$^+$CD45$^-$) or VE-cadherin$^-$CD45$^-$(VEcad$^-$CD45$^-$) cells were sorted on day 10. Representative FACS dot plots and percentages of gated cells are shown. Purities of viable VE-cadherin$^+$CD45$^-$ and VE-cadherin$^-$CD45$^-$ cells are 99.2% ± 0.6% and 99.9% ± 0.1%, respectively, from at least 3 independent experiments. (D) VE-cadherin$^+$ cells on day 10 were analyzed by FACS with various mAbs. Percentages of cells positive for each antigen among VE-cadherin$^+$ cells are shown. Gray line indicates isotype control; black line, VE-cadherin$^+$ cells. (E-J) Untransfected ESC-derived VE-cadherin$^+$CD45$^-$ cells sorted on day 10 were evaluated by the DiI-Ac-LDL incorporation assay (E) or immunostaining with IgG1 (F), anti–Hb (G), VEGFR-2 (H), eNOS (I), or VWF (J) Abs. Hoechst 33342 (E-J) and anti–VE-cadherin mAb (F-J) were used to detect nuclei and endothelial cells, respectively. Original magnification × 200. Scale bar, 50 μm.

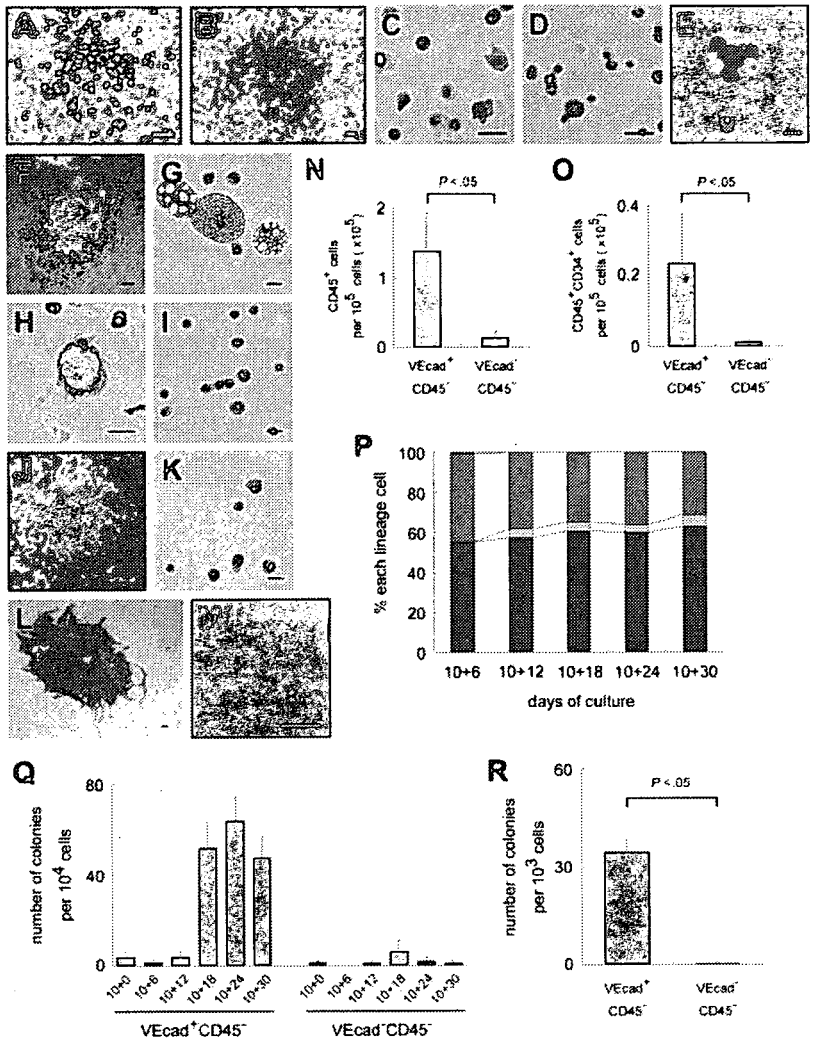

Figure 2. ESC-derived VE-cadherin$^+$CD45$^-$ cells generate hematopoietic and endothelial cells/colonies. Light micrographs of adherent hematopoietic clusters on days 10 + 5 (A) and 10 + 23 (B). (C-D) May-Giemsa staining of floating hematopoietic cells on days 10 + 6 (C) and 10 + 30 (D). (E) Immunostaining of floating hematopoietic cells on day 10 + 30 with anti–CD41 (red) and Hb (green) Abs. (F-K) Light micrographs and May-Giemsa staining of a GM (F-G), erythroid (H-I), or mixed colony (J-K) are depicted. (L) Immunostaining of an endothelial colony with anti–VE-cadherin mAb (blue). (M) Immunostaining of VE-cadherin$^+$CD45$^-$ cell-derived cells after 7-day culture with anti–VE-cadherin (red) and VWF (green) Abs. (E, M) Nuclei were labeled with Hoechst 33342. (N, O) Numbers of CD45$^+$ (N) or CD45$^+$CD34$^+$ cells (O) derived from 1 × 10^5 VE-cadherin$^+$CD45$^-$ (VEcad$^+$CD45$^-$) or VE-cadherin$^-$CD45$^-$ (VEcad$^-$CD45$^-$) cells. (P) Sequential analysis of the percentages of nucleated erythrocytes (red), enucleated erythrocytes (yellow), myeloid lineage cells (green), and megakaryocytes (blue) among floating cells. Each bar represents the mean of 3 independent experiments. (Q) Sequential analysis of the numbers of hematopoietic colonies per 1 × 10^4 VEcad$^+$CD45$^-$ or VEcad$^-$CD45$^-$ cell-derived cells. (R) Numbers of endothelial colonies per 1 × 10^3 VEcad$^+$CD45$^-$ or VEcad$^-$CD45$^-$ cells. (A-P) Data obtained from VEcad$^+$CD45$^-$ cells are shown. Data are presented as mean ± SD of 3 independent experiments in N-O and Q-R. Each experiment was performed in triplicate in P-R. Original magnification × 40 (B, F, L), × 100 (A, H, J), and × 200 (C-E, G, I, K, M). Scale bars, 20 μm (C-E, G, I, K), 50 μm (M), and 100 μm (A-B, F, H, J, L).

cells generated from the VE-cadherin$^+$CD45$^-$ population were 9.5- and 16.1-fold higher, respectively, than from the VE-cadherin$^-$CD45$^-$ population at day 10 + 7 ($P < .05$) (Figure 2N-O). It should be noted that VE-cadherin$^-$CD45$^-$ cells generated a small but significant minority of hematopoietic cells at day 10 + 7.

Floating hematopoietic cells emerged from the VE-cadherin$^+$CD45$^-$ population at approximately day 10 + 3. Their number was low until day 10 + 12 but increased exponentially afterward. Cells consisted exclusively of mature hematopoietic cells, such as erythrocytes, myeloid lineage cells, and megakaryocytes, as revealed by May-Giemsa staining and immunostaining (Figure 2C-E). Floating erythrocytes on day 10 + 6 were apparently larger than those on day 10 + 30 (Figure 2C-D). The percentage of erythrocytes among floating cells was approximately 60% to 70% throughout the experiments, which increased to some degree with time (Figure 2P). Enucleated erythrocytes accounted for less than 1% of total erythrocytes on day 10 + 6 and 6% to 10% from day 10 + 12 onward. Again, floating cells from the VE-cadherin$^-$CD45$^-$ population were rarely observed.

We also performed a sequential standard methylcellulose colony assay to evaluate the clonogenic potential of VE-cadherin$^+$CD45$^-$-derived or VE-cadherin$^-$CD45$^-$-derived cells. As shown in Figure 2Q, few colonies were generated from VE-cadherin$^+$CD45$^-$ cells (denoting day 10 + 0) and coculture of VE-cadherin$^+$CD45$^-$ cells on the OP9 layer for another 12 days (day 10 + 12), consisting exclusively of granulocyte-macrophage (GM) colonies. After 18 days of coculture (day 10 + 18), other colonies, including GM (Figure 2F-G), erythroid (Figure 2H-I), and mixed (Figure 2J-K), were detected. During the experiment, few colonies were generated from the coculture of VE-cadherin$^-$CD45$^-$ cells on the OP9 layer.

In endothelial differentiation cultures, sheetlike or cordlike VE-cadherin$^+$ endothelial colonies were generated after 7 days almost exclusively from the VE-cadherin$^+$CD45$^-$ population ($P < .05$) (Figure 2L, R). In 7-day culture, all endothelial cells had Ac-LDL uptake capacity and expressed VE-cadherin, VWF, VEGFR-2, CD31, CD34, and eNOS (Figure 2M and data not shown). Our results indicated that VE-cadherin$^+$CD45$^-$ cells isolated on day 10 composed a population of early endothelial cells with hemogenic properties that could differentiate into mature endothelial cells.

VE-cadherin$^+$CD45$^-$ population contains single cells with hematopoietic and endothelial capacities

We performed a single-cell deposition assay to analyze whether the VE-cadherin$^+$CD45$^-$ population contained common progenitors for hematopoietic and endothelial lineages. Individual wells of a 96-well plate were subjected to fluorescence microscopy 24 hours after cell deposition, and wells that contained more than one GFP$^+$ cell (ESC-derived cells) were excluded from subsequent analyses (5 of 2885 wells). Consistent with previous reports,[23] when a mixture of anti-CD45, CD41, and γ-globin mAbs was used, all

the round cells belonging to the hematopoietic lineage were stained positively.

Of the 2880 wells analyzed, 269 (8.6%) demonstrated clonal outgrowth consisting of endothelial progeny only (7.4%; 213 wells) (Figure S1A, available on the *Blood* website; see the Supplemental Figures link at the top of the online article), hematopoietic progeny only (0.17%; 5 wells) (Figure S1B), and both endothelial and hematopoietic progeny (1.1%; 31 wells) (Figure S1C). Thus, our results clearly demonstrated that the VE-cadherin$^+$CD45$^-$ population contained common progenitors for hematopoietic and endothelial lineages.

VE-cadherin$^+$CD45$^-$ cells generated primitive and definitive erythrocytes sequentially

To determine whether the erythrocytes derived from the VE-cadherin$^+$CD45$^-$ population were primitive or definitive, we analyzed the expression patterns of embryonic (ζ and ε), fetal (α and γ), and adult (β) globins in floating erythrocytes by sequentially immunostaining for various globin chains (Figure 3). Until day 10 + 6, all floating erythrocytes expressed ε- and ζ-globins, whereas β-globin expression was hardly detected (less than 1%). The percentage of floating erythrocytes positive for β-globin increased gradually from day 10 + 12, and almost all erythrocytes were positive by day 10 + 30. Meanwhile, expression of ε- and ζ-globins declined gradually to approximately 90% and 80% by day 10 + 30, respectively. All floating erythrocytes expressed α- and γ-globins throughout the experimental period. Others and we have found β-globin the most specific type of globin genes for the identification of definitive erythrocytes.[4,25,29,30,34] Results here showed that β-globin, a specific marker for definitive erythrocytes,

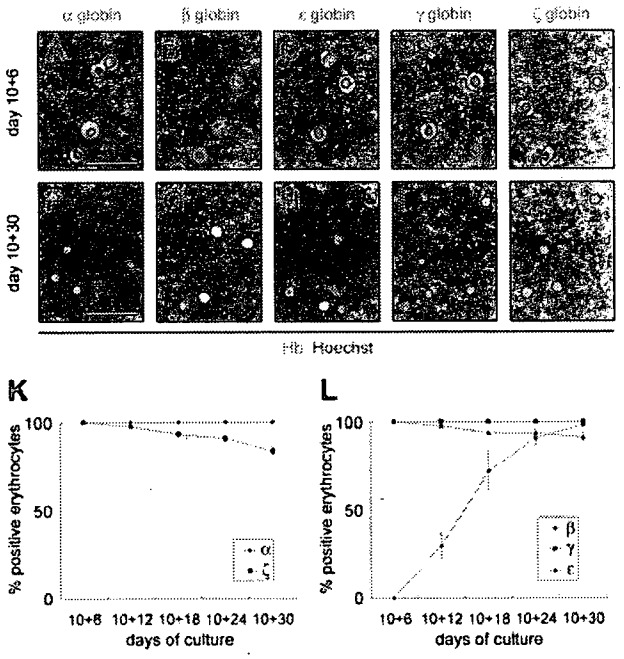

Figure 3. ESC-derived VE-cadherin$^+$CD45$^-$ cells generate primitive and definitive erythrocytes sequentially. Immunostaining of floating erythrocytes on days 10 + 6 (A-E) and 10 + 30 (F-J). Cy3 detection of erythrocytes stained with anti–α-, anti–β-, anti–ε-, anti–γ-, or anti–ζ-globin mAbs (red) and FITC detection with anti–Hb polyclonal Ab (green). Anti-Hb Ab, which reacts with embryonic, fetal, and adult erythrocytes, was used to detect all erythrocytes. Nuclei were labeled with Hoechst 33342. Merged images are shown. Original magnification × 200. Scale bars, 50 μm. (K-L) Sequential analysis of the proportion of erythrocytes positive for anti–α- or anti–ζ-globin mAbs (K) and anti–β-, anti–γ-, or anti–ε-globin mAbs (L) among the total erythrocytes. Data are presented as mean ± SD of 3 independent experiments.

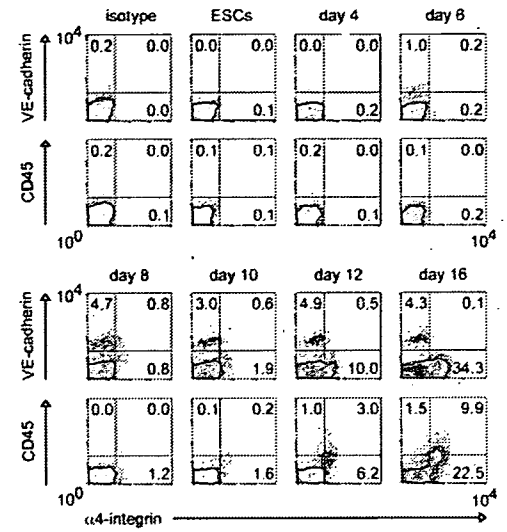

Figure 4. Temporal emergence of VE-cadherin$^+$α4-integrin$^+$ cells during ESC differentiation. As described for Figure 1, undifferentiated GFP-transfected ESCs and subsequent differentiating cells were analyzed by FACS. Percentages of cells in each quadrant among the total viable GFP$^+$ cells are indicated. Representative results from 1 of 3 independent experiments are shown.

is up-regulated gradually in the OP9 coculture and that VE-cadherin$^+$CD45$^-$ cells generate primitive and definitive erythrocytes sequentially.

Hematopoietic progenitors exclusively reside in the α4-integrin$^+$ subpopulation of VE-cadherin$^+$CD45$^-$ cells

In vivo and in vitro experiments in mice show that α4-integrin is a marker of the earliest precursor of hematopoietic cell lineage from endothelial progenitors.[26] To determine whether this is applicable to primates, we sequentially traced the expression patterns of VE-cadherin, CD45, and α4-integrin in differentiating ESCs cocultured with OP9 cells. As shown in Figure 4, VE-cadherin$^+$α4-integrin$^+$ cells first appeared on day 6, peaked at approximately days 8 to 10, and almost disappeared by day 16. In contrast to the previously reported time-course of mouse ESC differentiation,[26] VE-cadherin$^+$ and α4-integrin$^+$ cells simultaneously developed from monkey ESCs. CD45$^+$ cells appeared from day 12 onward, and most coexpressed α4-integrin.

Next, we isolated VE-cadherin$^+$α4-integrin$^-$, VE-cadherin$^+$α4-integrin$^+$, and VE-cadherin$^-$α4-integrin$^+$ cells on day 10 after excluding dead cells and CD45$^+$ cells to evaluate their hematopoietic and endothelial capacity (Figure 5A). Isolated cells were reseeded onto fresh confluent OP9 layers and were cultured with hematopoietic cytokine mixture. Among the VE-cadherin$^+$CD45$^-$ population, only the α4-integrin$^+$ subpopulation gave rise to adherent hematopoietic clusters and floating hematopoietic cells (Figure 5C, F, H). Adherent clusters grew, and the number of floating cells increased throughout the experimental period (Figure 5D, G-H). VE-cadherin$^+$α4-integrin$^+$ cells generated 5- to 10-fold more floating hematopoietic cells than total VE-cadherin$^+$ cells. VE-cadherin$^-$α4-integrin$^+$ cells yielded more adherent clusters and floating cells than VE-cadherin$^+$α4-integrin$^+$ cells until day 10 + 6 (Figure 5B, E). Interestingly, however, the adherent clusters from VE-cadherin$^-$α4-integrin$^+$ cells disappeared by day 10 + 12, and the number of floating cells declined drastically (Figure 5H). Again, the sizes of floating erythrocytes on day 10 + 6 derived from VE-cadherin$^+$α4-integrin$^+$ and VE-cadherin$^-$α4-integrin$^+$ cells were larger than those on day 10 + 30 from VE-cadherin$^+$α4-integrin$^+$ cells (Figure 5E-G).

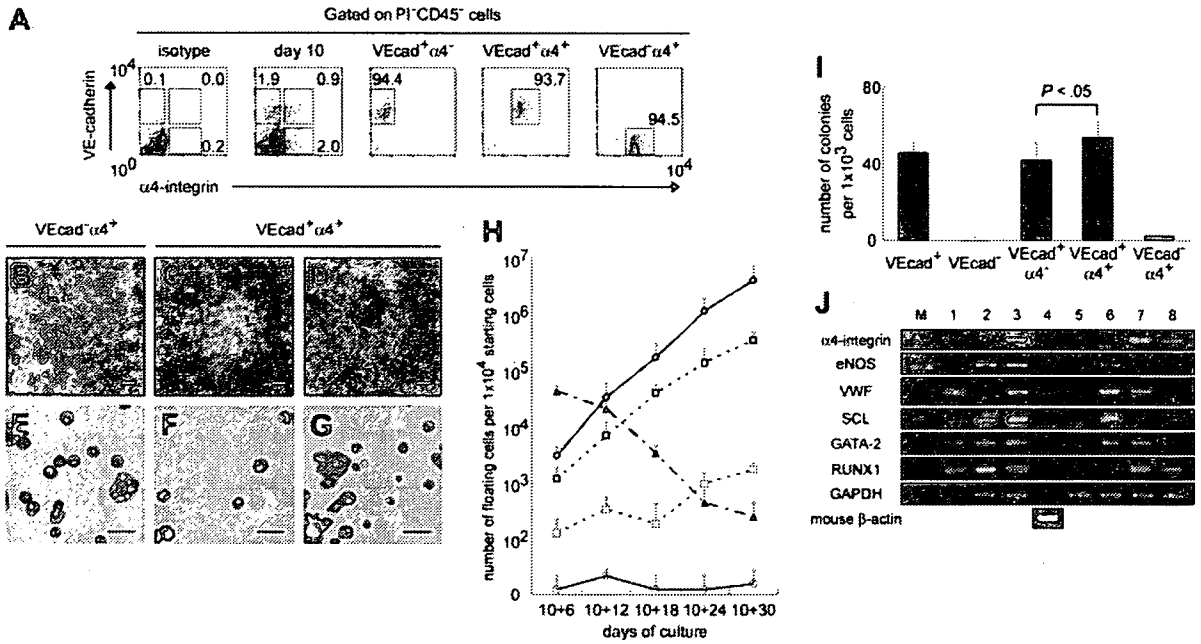

Figure 5. Hematopoietic progenitors exclusively reside in the α4-integrin⁺ subpopulation among VE-cadherin⁺CD45⁻cells. (A) VE-cadherin⁺α4-integrin⁻ (VEcad⁺α4⁻), VE-cadherin⁺α4-integrin⁺ (VEcad⁺α4⁺), or VE-cadherin⁻α4-integrin⁺ (VEcad⁻α4⁺) cells were sorted on day 10 after the exclusion of PI⁺ and CD45⁺ cells. Representative FACS dot plots and percentages of gated cells are shown. Purities of viable VEcad⁺α4⁻, VEcad⁺α4⁺, and VEcad⁻α4⁺ cells are 95.0%± 3.0%, 94.1%± 0.5%, and 96.9%± 2.1%, respectively, from at least 3 independent experiments. (B-D) Light micrographs of adherent hematopoietic clusters on day 10 + 6 from VEcad⁻α4⁺ cells (B) and days 10 + 6 (C) and 10 + 18 (D) from VEcad⁺α4⁺ cells. (E-G) May-Giemsa staining of floating hematopoietic cells on day 10 + 6 from VEcad⁻α4⁺ cells (E) and days 10 + 6 (F) and 10 + 30 (G) from VEcad⁺α4⁺ cells. Original magnification × 40 (B-D) and × 200 (E-G). Scale bars, 100 μm (B-D) and 20 μm (E-G). (H) Sequential analysis of the numbers of floating viable cells per cultured 1 × 10⁴ VE-cadherin⁺ (▣), VE-cadherin⁻ (□), VEcad⁺α4⁻ (○), VEcad⁺α4⁺ (●), or VEcad⁻α4⁺ (▲) cells. (I) Numbers of endothelial colonies per 1 × 10³ cells in each subpopulation. (H-I) Data are presented as mean ± SD of 3 independent experiments. Each experiment was performed in triplicate. (J) RT-PCR analysis of genes associated with hematopoietic or endothelial development. Each lane contained cDNA from the following cells: adult cynomolgus monkey BM cells (lane 1), K562 erythroblastic cells (lane 2), human umbilical vein endothelial cells (lane 3), OP9 stromal cells (lane 4), total GFP⁺ ESC-derived cells (lane 5), VE-cadherin⁺α4-integrin⁻ cells (lane 6), VE-cadherin⁺α4-integrin⁺ cells (lane 7), and VE-cadherin⁻α4-integrin⁺ cells (lane 8) sorted on day 10. Representative results from 1 of 3 independent experiments are shown.

To clarify the difference in hematopoietic kinetics between VE-cadherin⁺α4-integrin⁺ and VE-cadherin⁻α4-integrin⁺ populations, we examined whether floating erythrocytes derived from each population were primitive or definitive. As in the VE-cadherin⁺CD45⁻ population, all floating erythrocytes derived from both populations expressed α-, ϵ-, γ-, and ζ-globins but were devoid of β-globin on day 10 + 6 (Figure S2A-E, K-O), indicative of primitive erythrocytes. Moreover, almost all erythrocytes from the VE-cadherin⁺α4-integrin⁺ population were positive for β-globin by day 10 + 30, whereas the expression of ϵ- and ζ-globins declined gradually (Figure S2F-J), characteristic of definitive erythrocytes.

In endothelial differentiation cultures with VEGF, VE-cadherin⁺α4-integrin⁺ cells generated significantly more endothelial colonies than VE-cadherin⁺α4-integrin⁻ cells after 7-day culture ($P < .05$) (Figure 5I). VE-cadherin⁻α4-integrin⁺ cells barely generated endothelial colonies.

To verify the hematopoietic and endothelial capacities of these 3 populations, gene expression profiles were investigated with the use of RT-PCR (Figure 5J). The presence of α4-integrin was confirmed specifically in the VE-cadherin⁺α4-integrin⁺ and VE-cadherin⁻α4-integrin⁺ populations. *eNOS* and *VWF*, representative endothelial proteins, were expressed in VE-cadherin⁺α4-integrin⁻ and VE-cadherin⁺α4-integrin⁺ populations, whereas *VWF* was expressed weakly in the VE-cadherin⁻α4-integrin⁺ population. *SCL* and *GATA-2*, transcriptional factors associated with hematopoietic and endothelial development,[38,39] were expressed in all 3 populations. Notably, *RUNX1*, a transcriptional factor associated with definitive hematopoiesis,[40,41] was expressed in the VE-cadherin⁺α4-integrin⁺ and VE-cadherin⁻α4-integrin⁺ populations but not in VE-cadherin⁺α4-integrin⁻ cells.

Finally, we performed a single-cell deposition assay of VE-cadherin⁺α4-integrin⁺ cells. We differentiated GFP-transfected ESCs, and single VE-cadherin⁺α4-integrin⁺ cells that were exclusively negative for CD45 were assayed on day 10. Of the 958 wells analyzed (2 of 960 wells were omitted because they contained more than 1 GFP⁺ cell), 106 (11.1%) demonstrated clonal outgrowth consisting of endothelial progeny only (6.3%; 60 wells), hematopoietic progeny only (0.52%; 5 wells), and both endothelial and hematopoietic progeny (4.3%; 41 wells). Hence, common progenitors for hematopoietic and endothelial lineages in the VE-cadherin⁺CD45⁻ population were 4.0-fold more enriched in the α4-integrin⁺ subpopulation ($P < .001$).

Thus, these results suggested that among VE-cadherin⁺CD45⁻ cells, only the α4-integrin⁺ subpopulation participated in primitive and definitive hematopoiesis, whereas α4-integrin⁺ and α4-integrin⁻ subpopulations were involved in endothelial lineage development. Our results also showed that VE-cadherin⁻CD45⁻α4-integrin⁺ and VE-cadherin⁺CD45⁻α4-integrin⁺ cells were primary sources for primitive and definitive hematopoiesis, respectively.

Colonies consisting of primitive and definitive erythrocytes are generated from VE-cadherin⁺α4-integrin⁺ cells

As shown, erythroid colonies were not generated from VE-cadherin⁺CD45⁻ cells by day 10 + 18 with the standard methylcellulose assay (Figure 2Q). Others and we[24,42] have reported the successful development of colonies consisting of primitive erythrocytes on OP9 stromal layers. Colony-forming assays were performed on OP9 layers. Colonies consisting of

primitive erythrocytes were generated after 7-day coculture on OP9 cells from the VE-cadherin$^+$, VE-cadherin$^+$α4-integrin$^+$, and VE-cadherin$^-$α4-integrin$^+$ populations but not the VE-cadherin$^+$α4-integrin$^-$ population (Figure 6A-D, I). All erythrocytes in individual colonies from these populations were positive for ζ-globin but devoid of β-globin, indicative of primitive erythrocytes. The primitive erythroid clonogenic progenitors in the VE-cadherin$^+$ population were 8.7-fold more enriched in the α4-integrin$^+$ subpopulation (Figure 6I). On the other hand, the VE-cadherin$^-$α4-integrin$^+$ population yielded a significantly higher number of colonies consisting of primitive erythrocytes and GM than the VE-cadherin$^+$α4-integrin$^+$ population (each $P < .05$), analogous to the patterns for floating hematopoietic cells in both populations (Figure 5H). We used the standard methylcellulose assay to generate colonies consisting of definitive erythrocytes after day 10 + 18 from the VE-cadherin$^+$ and VE-cadherin$^+$α4-integrin$^+$ populations but not the VE-cadherin$^+$α4-integrin$^-$ and VE-cadherin$^-$α4-integrin$^+$ populations (Figure 6E-H, J). All erythrocytes in individual colonies were positive for β-globin, and some were devoid of ζ-globin, characteristic of definitive erythrocytes.

Thus, the VE-cadherin$^+$α4-integrin$^+$ population displayed primitive and definitive erythroid clonogenic activity. Our data showed that hemogenic endothelial cells are not only the sole progenitor population for definitive hematopoiesis, they are deeply involved in primitive hematopoiesis.

Discussion

Despite several similarities, a number of differences were observed between mouse and primate hematopoietic development, such as the pattern of globin switching during the shift of hematopoietic sites. To clarify the pathogenesis and treatment of hematologic disorders in humans, it was important to investigate hematopoietic development using primate materials. In the near future, it may be necessary to apply human ESC-derived products to nonhuman primates as preclinical models for cell transplantation, ahead of their use in clinical settings. However, relatively little is known about hematopoiesis during primate embryogenesis compared with mouse embryogenesis, partly because of poor availability and ethical limitations of primate embryos. Thus, primate ESCs are more promising for studies on primate embryogenesis. In addition, coculture with the OP9 stromal cells has been used successfully for hematopoietic differentiation of mouse and primate ESCs.[23,24,31,42,43] In this report, we used the primate ESC and OP9 coculture system and demonstrated for the first time that α4-integrin$^+$ hemogenic endothelial cells are deeply involved in primitive and definitive hematopoiesis in primates.

Sequential development of primitive and definitive hematopoiesis from ESC-derived endothelial cells

We showed that VE-cadherin$^+$CD45$^-$ endothelial cells derived from nonhuman primate ESCs generate primitive and definitive erythrocytes. To date, several studies demonstrate hematopoietic differentiation of human and nonhuman primate ESCs.[23,24,34,43-46] Previous in vivo and in vitro experiments in humans indicate that at least a proportion of hematopoietic cells originate in vascular endothelial cells.[12,45] However, whether primitive hematopoiesis and definitive hematopoiesis originate in hemogenic endothelium in primates remains to be elucidated. Data obtained in mice are controversial. Numerous investigators report that only multilineage definitive, but not primitive, hematopoietic progenitors arise from

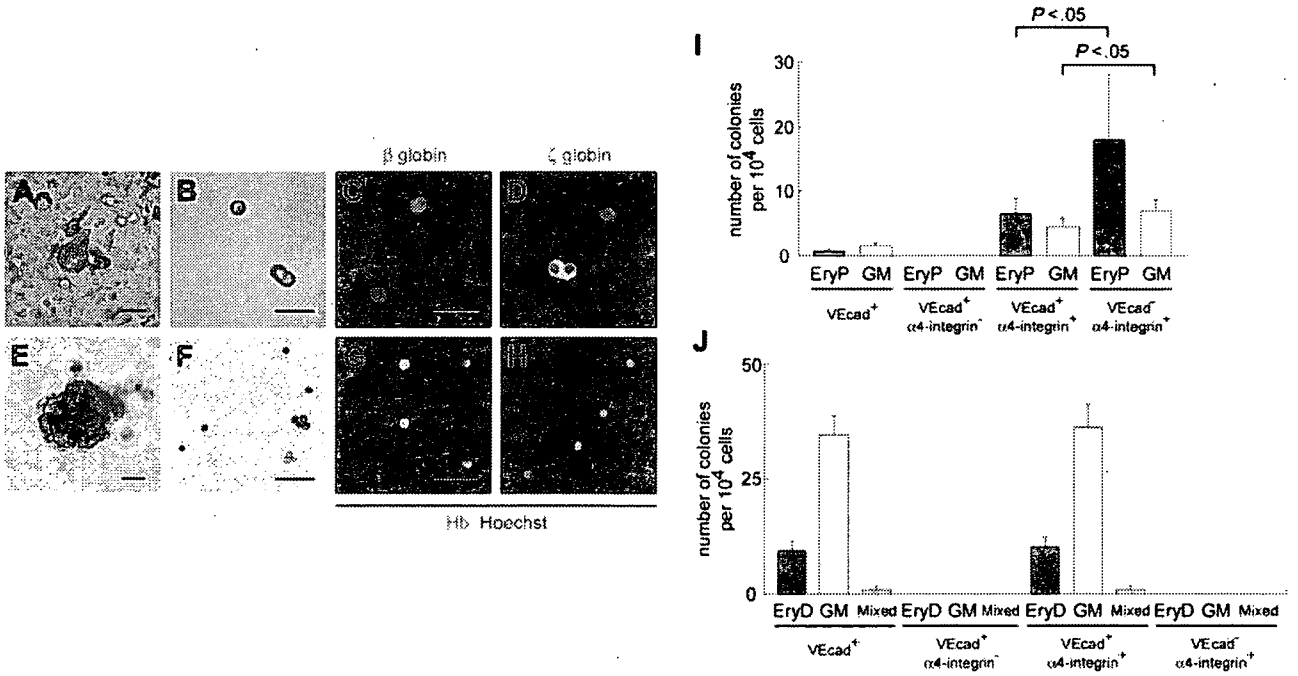

Figure 6. α4-Integrin$^+$ subpopulation among VE-cadherin$^+$CD45$^-$ cells generates hematopoietic colonies composed of primitive and definitive erythrocytes. (A-H) Light micrographs and May-Giemsa staining of colonies consisting of primitive (A-B) and definitive (E-F) erythrocytes from VE-cadherin$^+$α4-integrin$^+$ cells are depicted. Immunostaining data from colonies consisting of primitive (C-D) and definitive (G-H) erythrocytes from VE-cadherin$^+$α4-integrin$^+$ cells are also presented. Cy3 detection of erythrocytes stained with anti–β-globin (C, G) or anti–ζ-globin (D, H) mAbs (red) and FITC detection with anti-Hb polyclonal Ab (green). Nuclei were labeled with Hoechst 33342. Merged images are shown. Original magnification × 100 (A, E) and × 200 (B-D, F-H). Scale bars, 50 μm. (I-J) Numbers of hematopoietic colonies per 1 × 10^4 cells sorted on day 10 (I) or after 30-day coculture on OP9 layers (J) in each subpopulation. VEcad$^+$ denotes the VE-cadherin$^+$CD45$^-$ population. EryP and EryD represent colonies consisting of primitive and definitive erythrocytes, respectively. Data are presented as mean ± SD of 3 (I) or 2 (J) independent experiments. Each experiment was performed in duplicate (I) or triplicate (J).